

# Reference Cavity Design Considerations\*

WILLIAM A. GERARD†

**Summary**—The design problems in a reference cavity include coupling, cavity  $Q$ , temperature compensation, stability, and hysteresis. Temperature compensation is shown to be a problem in second order compensation theory and is solved by material changes. Stability is achieved by novel mechanical design and by elimination of hysteresis producing members.

## REFERENCE CAVITY DESIGN CONSIDERATIONS

THE 1Q SERIES reference cavity has held a unique place in the field of microwave devices. It has remained virtually unchanged in over 10 years of use. The introduction of the standing-wave discriminator has created a need for cavities matched to waveguide impedance with bandwidth and transmission characteristics of the 1Q retained. Furthermore a demand has arisen for a frequency standard that would maintain frequency at very low temperatures. The problem then resolved itself to what can be done that will result in a major improvement in compensation and stability on the 1Q.

## THE MATCHING PROBLEM

The desirability of a matched cavity for the standing-wave discriminator has been demonstrated by Denton, Wilson, and Margolin.<sup>1</sup> Their results show that maximum sensitivity results when the cavity is matched to the waveguide. The scheme of operation is shown in Fig. 1. As generator frequency changes, the vswr pattern shifts and increases in amplitude. Two crystals are located symmetrically about the position of vswr minimum, and, when the pattern shifts, there is an unbalance which is used to actuate a feedback system. This in turn is used to correct the generator frequency.

To match the 1Q series reference cavity, a study was undertaken in which the windows were varied in size and the measured coupled characteristics of the cavity were compared with the theoretical characteristics of an ideal cavity. Plots of the coupled characteristics of a 1Q are shown in Fig. 2 and the characteristics of an ideal cavity<sup>2</sup> are shown in Fig. 3 (both opposite). The latter is plotted in terms of the coupling parameters  $B_1$  and  $B_2$ , the former in terms of actual window diameters. The window diameters are directly related to the  $B$  parameters. Comparison of the curves shows general similarity, the major difference being that the unloaded  $Q$  in an ac-

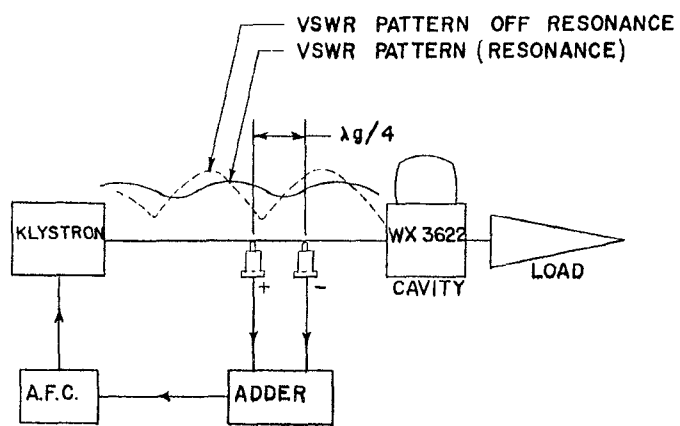


Fig. 1—Standing-wave discriminator.

tual cavity changes as windows are opened. The measured curves for the 1Q cavity were obtained by selecting several cavities with similar characteristics (especially unloaded  $Q$ ) and successively machining the windows. The cavity was degreased after each machining operation to eliminate oil films which would otherwise cause poor results. The theoretical curves show that if an input match better than 1.4 is to be achieved with the same transmission fraction ( $T$ ) as the 1Q (equivalent to 5 db insertion loss), a  $Q$  of 1650 would result.

The present design of the 1Q was dictated by considerations developed by Pound,<sup>3</sup> where maximum sensitivity for a transmission system is shown to be obtained when the cavity has equal input and output coupling. For a cavity with fixed unloaded  $Q$ , this results in a maximum  $TQ_L$  product. Obviously the matched 1Q will no longer exhibit the same  $TQ_L$  product since the matched cavity for fixed transmission fraction has a lower  $Q_L$ . The lower  $Q_L$  would also lower the sensitivity of the standing-wave discriminator. The best solution would be to raise the unloaded  $Q$  from the 5000 of the 1Q design to about 6500 where both applications could be served with equal ease.

## UNLOADED $Q$

To understand the unloaded  $Q$  changes contemplated, it is helpful to examine the nature of the mode used in the 1Q. Barrow and Mieher<sup>4</sup> have sketched the effect of the addition of a rod or nose on the perfect cylindrical  $TM_{010}$  mode.

\* Manuscript received by the PGMTT, October 5, 1956.

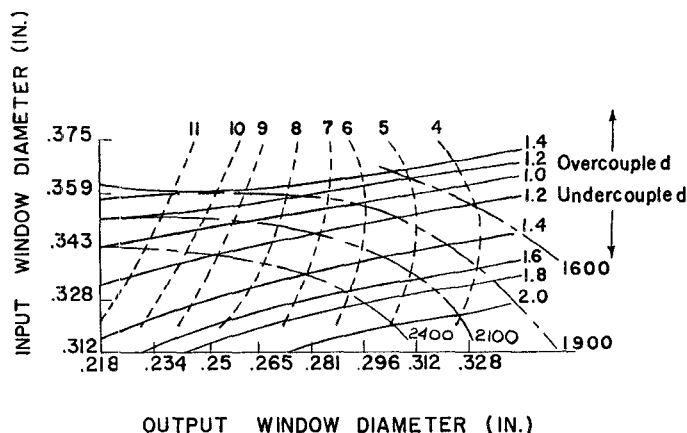
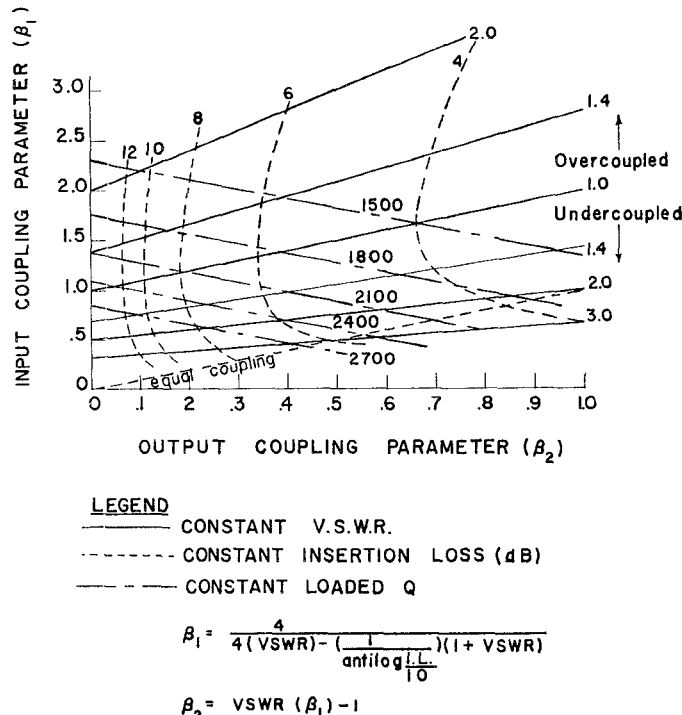
† Westinghouse Electric Corp., Horseheads, N. Y.

<sup>1</sup> R. F. Denton, T. A. Wilson, and A. R. Margolin, "Automatic Frequency Control of High-Power Klystron," N.E.C., Chicago, Ill., 1952.

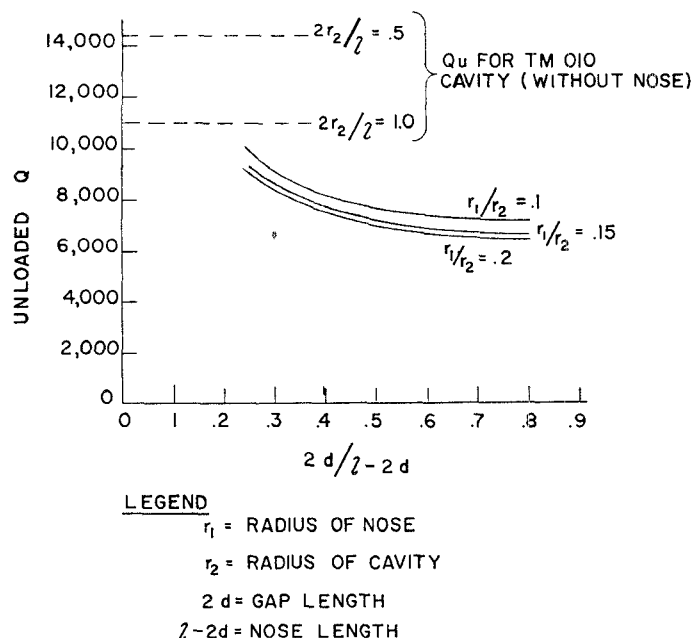
<sup>2</sup> C. G. Montgomery, "Technique of Microwave Measurements," vol. 11, M.I.T. Rad. Lab. Ser., McGraw-Hill Book Co., New York, N. Y., pp. 286-291.

<sup>3</sup> R. V. Pound, "Microwave Mixers," vol. 16, M.I.T. Rad. Lab. Ser., pp. 215-218.

<sup>4</sup> W. L. Barrow and W. W. Mieher, "Natural oscillations of electrical cavity resonators," PROC. IRE, vol. 28, pp. 184-191; April, 1940.

Fig. 2—Coupled properties of 1Q cavity.  $f=9280$  mc.Fig. 3—Coupled properties of an ideal cavity.  $Qu=5000$ .

The 1Q series cavity uses a configuration that is much closer to the  $TM_{010}$  mode than to the  $TM_{001}$  capacity loaded coaxial mode that has been more widely treated due to its application to klystron design. The desirable feature of the nosed-in cavity is that the presence of the nose provides a high tuning rate for compensation purposes. The nose, however, will lower the  $Q$  as compared to the associated  $TM_{010}$  cavity. This is borne out in Fig. 4, which gives the relative  $Qu$  values for nosed-in cavities as a function of their geometry. Frequency is held constant. To calculate the frequency to a sufficient

Fig. 4—Unloaded  $Q$  for nosed-in cavity. Material—copper.

accuracy (1 per cent) for the geometries of greatest interest, it was necessary to extrapolate the curves given by Holstein and Mayer.<sup>5</sup> The  $Q$  values were calculated from a method given by Warnecke and Guenard<sup>6</sup> for nosed-in cavities in the capacity loaded coaxial mode. The legitimacy of

$$Qu = 4\pi^{3/2} \cdot 10^{-7} f^{1/2} \sigma^{1/2} \mu^{-1/2} K \frac{(r_2^2 - r_1^2)l + r_1^2 2d}{[r_2(r_2 - 1) + r_1(l - 2d)]}$$

$$u = 4 \times 10^{-7}$$

$\sigma$  = conductivity

$f$  = frequency

$$K = \text{geometric parameter} = \frac{1/V \iiint H^2 dV}{1/S \iint H^2 dS}$$

(approximately unity, also see Fig. 134 of footnote 6)

$r_1, r_2, l, 2d$  = cavity dimensions, [Fig. 5(a) next page]

the use of their formula is justified by comparison with the value of  $Qu$  computed for nearly equivalent  $TM_{010}$  cavities and by subsequent experiment. Fig. 4 shows that the final choice of geometry thus represents a compromise between tuning rate, size, and  $Qu$ .

These curves give a  $Qu$  of 6800 for the 1Q while measurements yield a  $Qu$  of 5000. Studies of the various surface conditions and assembly techniques were under-

<sup>5</sup> T. Holstein and E. Mayer, "Resonant Frequencies of the Nosed-in Cavity," Westinghouse Electric Corp., Res. Rep. SR-281.

<sup>6</sup> R. Warnecke and P. Guenard, "Tubes Electronique à Modulation de Vitesse," Gauthier-Villars, Paris, France, p. 234.

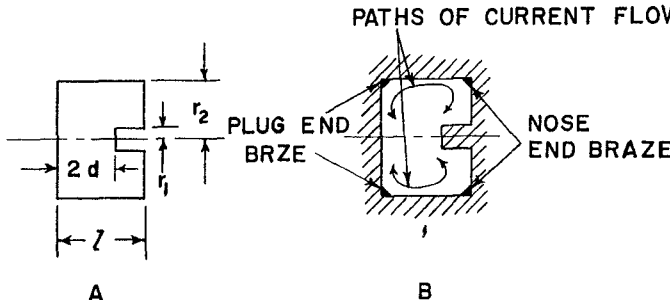


Fig. 5—Nosed-in cavity nomenclature and assembly.

taken to see whether higher  $Q$  could be obtained in practice. Tests showed that the smoother side wall surface obtained by ball-burnishing was no better than a machined side wall. The corrugated diaphragm was equally as good as a smooth machined surface. The chief loss of  $Q$  that could be improved by changing fabrication technique was in the braze joints. Poor joints resulted in extremely low  $Q$  values because cavity currents flow perpendicular to these joints. Even the best of joints using silver-copper eutectic solder resulted in a substantial loss of  $Q$ . A special set of cavities was constructed that were machined in different fashions. Referring to Fig. 5(b) and Table I we can see that the

TABLE I

$Qu$	
6380	brazes at both ends
7120	
7320	nose end brazes only
7800	
7340	plug end brazes only
8250	

elimination of at least one braze joint made a substantial contribution to the unloaded  $Q$  of a WX-3622 cavity having a theoretical unloaded  $Q$  of 9000. Cavities made with joints parallel to the path of current flow showed almost no reduction of  $Q$ , but construction of this type is difficult. The size of the coupling holes affected  $Qu$  but the size ultimately is dictated by the coupled characteristics of the cavity. The input and output windows also decreased the unloaded  $Q$  by adding dielectric loss. This was substantially eliminated by the use of 7070 glass.

#### TEMPERATURE COMPENSATION

The theory of 2nd order compensation has been treated by Wheeler.<sup>7</sup> We may review these results before applying them to this compensation problem. If cavity wavelength scales linearly with change in dimension, we may write cavity frequency as a function of temperature.

$$\Delta f = -f_0(\alpha_1 \Delta t + \beta_1 \Delta t^2)$$

<sup>7</sup> M. S. Wheeler, "Tunable temperature compensated reference cavity," *Wireless Eng.*, vol. 32, pp. 201-205; August, 1955.

where

$\Delta f$ =frequency change in mc

$f_0$ =resonant frequency

$\Delta t$ =change in temperature in  $^{\circ}\text{C}$

$\alpha_1, \alpha_2$ =1st order coefficients of thermal expansion

$\beta_1, \beta_2$ =2nd order coefficients of thermal expansion.

As shown in Fig. 7, we may then introduce a tuner of length  $L$  (of a second metal having expansion coefficients  $\alpha_2, \beta_2$ ) which has a tuning rate of  $R$  mc per mil. Then

$$\begin{aligned} \Delta f = & -f_0(\alpha_1 \Delta t + \beta_1 \Delta t^2) \\ & + RL\{(\alpha_2 - \alpha_1)\Delta t + (\beta_2 - \beta_1)\Delta t^2\}. \end{aligned}$$

If we multiply through by  $1/\Delta t$  and setting  $\Delta f/\Delta t$  equal to 0, we obtain the equation of 1st order compensation.

$$\begin{aligned} 0 = \frac{\Delta f}{\Delta t} = & -f_0\alpha_1 + RL(\alpha_2 - \alpha_1) \\ & + \text{second order terms } [-f_0\beta_1 + RL(\beta_2 - \beta_1)]\Delta t. \\ = & -f_0\alpha_1 + RL(\alpha_2 - \alpha_1). \end{aligned}$$

When  $RL$  is made equal to  $f_0\alpha_1(\alpha_2 - \alpha_1)$  the first order error is zero. Using this value of  $RL$  in the original expression will give us the residual shift that can not be eliminated by a bimetal.

$$\Delta f = f_0 \Delta t^2 \frac{(\alpha_1 \beta_2 - \alpha_2 \beta_1)}{(\alpha_2 - \alpha_1)}.$$

The resulting equation shows that for a given temperature change, the change in frequency is a function of the material properties only. An examination of Fig. 6 shows that copper can be best compensated with iron, but the resulting bimetal would be too long due to the small difference in  $\alpha$  values. These curves should serve as a guide as actual materials do not behave precisely as the published expansion figures. Many of these curves, however, were confirmed by measurements on uncompensated cavities. The concave upward characteristic of tungsten will be shown to be desirable for it will compensate for nonlinearities in the tuning rate ( $R$ ) characteristic. The tungsten compensator will fit the nosed-in cavity compensation requirements nicely since a low expansion system moving the nose would compensate a copper cavity. This is most fortunate since tungsten is easily fabricated in rod form. If we were required to work with a  $\text{TE}_{111}$  cavity, for example, we would be required to attach the copper to one side wall and make the cavity body out of tungsten.

Several configurations could be considered as possible alternate designs for a nosed-in cavity. Referring to Fig. 7, configuration #1 is essentially the  $1Q$  structure with a tungsten strut substituted for the invar. This design shows pronounced hysteresis (changes in room temperature frequency with temperature cycling) and requires a high conductivity plating on the tungsten.

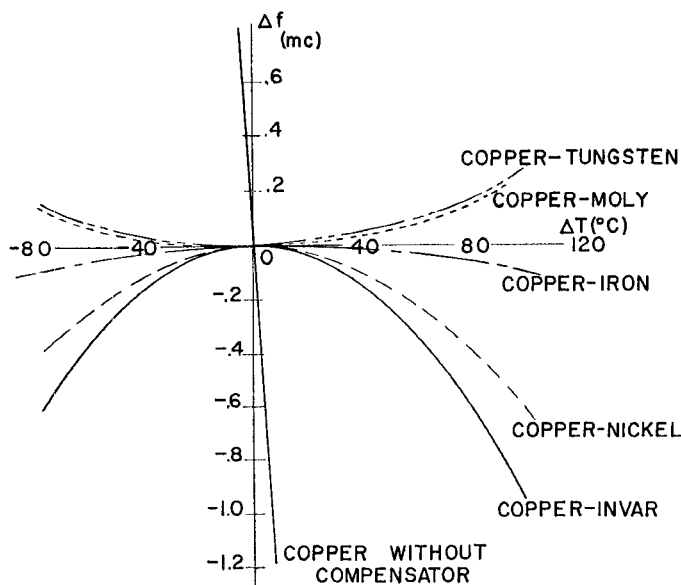


Fig. 6—Residual temperature compensation.

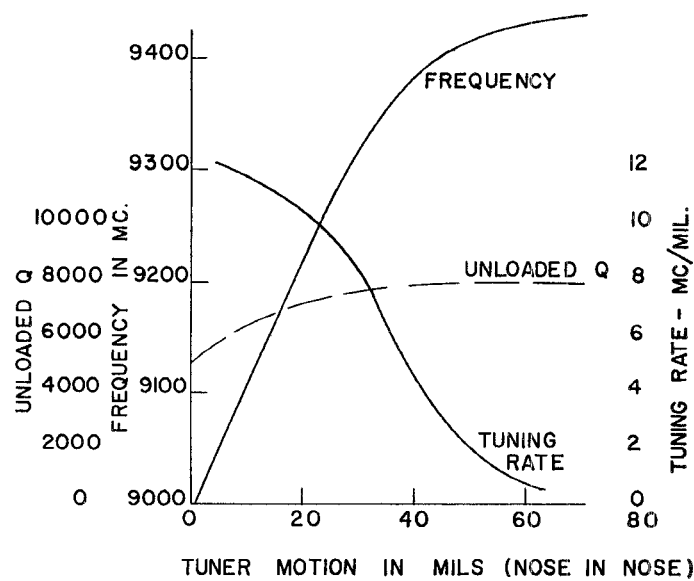
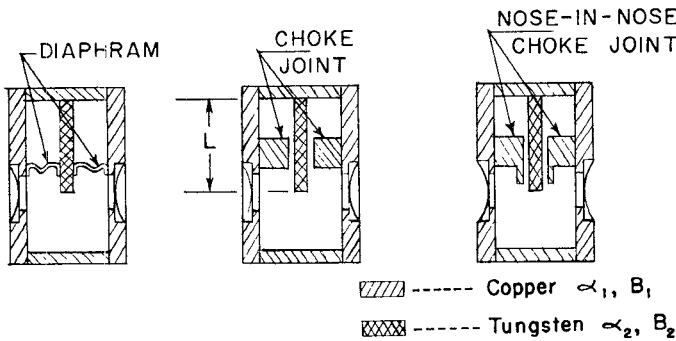
Fig. 8—Tuning rate and  $Q_u$  for nose-in-nose cavity

Fig. 7—Nosed-in cavity configurations

The portion of the tuner within the cavity might have been made of copper but this would have increased the over-all size. The hysteresis is the result of cold working the diaphragm during temperature cycling. This has been measured as high as 0.4 mc for a 9280 mc cavity. Configuration #2 offers a method of eliminating diaphragm hysteresis by use of a choke joint to allow the bimetallic action. Unfortunately, the nose plating is still a problem, and the design has low unloaded  $Q$  due to the break in the cavity wall. The base of the nose is a high current point. The choke would be better located as it is in configuration #3 where a nose-in-nose structure is chosen. Here the choke joint is located close to the current zero which appears at the center of the end of the nose. This design offers greater latitude in choke joint design and the nose plating problem is eased due to the smaller current flowing over it.

Fig. 8 shows the tuning properties and unloaded  $Q$  for a cavity with a nose-in-nose configuration. As the inner nose is advanced into the cavity, tuning rate increases as frequency and unloaded  $Q$  decrease. The tuning rate  $R$  is chosen depending on the compensator

length that can be used, over-all size being the determining factor. A typical value might be 9.4 mc/mil. Note the nature of the tuning rate curve in terms of compensator action. As the cavity system is heated, the inner nose is withdrawn by the bimetal to compensate. However, the tuning rate decreases as the inner nose is withdrawn. When the cavity is cooled, the opposite effect takes place. This has the effect of adding first order error to the curve for copper-tungsten shown in Fig. 6. The net effect is to pull the concave upward into one that is concave downward. This is shown in Fig. 10 to be less than 0.1 mc from  $-55^{\circ}\text{C}$  to  $+71^{\circ}\text{C}$ . The nonlinearity of the tuning rate may be used to advantage to adjust the value of compensation on individual cavities.

The Westinghouse WX3622 cavity was developed along the lines of thought described above. It is a tungsten compensated copper cavity which is evacuated and sealed. The mechanical isolation from the waveguide of the 1Q series<sup>8</sup> was preserved by holding the cavity in an aluminum block with thin mounting rings. The input vswr was held to 1.4 max, with transmission fraction  $\frac{1}{4}$ , and loaded  $Q$  2100 to 2400. To insure the accuracy of the compensation and frequency setting, considerable work was done to improve present frequency measuring systems. Great pains were taken to match the test systems. The most important improvement was the change in presentation technique. By use of an electronic switch, the cavity response was placed on the scope along with the swept klystron mode. This allows accurate tuning of the klystron. Improper "peaking" of the klystron turned out to be a chief source of error in previous work. Pulses are generated by beating

<sup>8</sup> D. Alpert *et al.*, U.S. Patent No. 2,584,717.

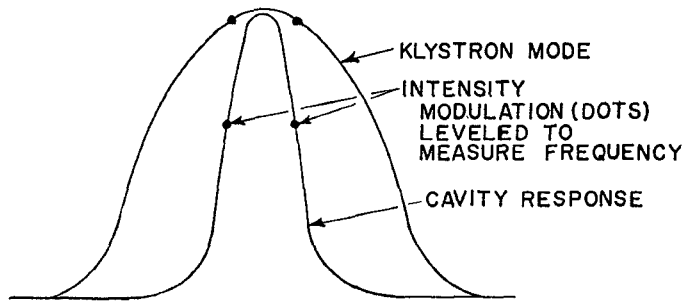


Fig. 9—Oscilloscope trace for frequency measurement.

a standard frequency harmonic against the swept klystron. The pulses become intensity modulation (dots) on the scope and frequency is measured by leveling these dots. It can be seen in Fig. 9 that if the klystron is tuned so that cavity frequency is on the sloping portion of the characteristic, an error will result in frequency reading. Present technique calls for leveling the dots on both the cavity response and on the klystron mode. Under these conditions equal power at the measurement level is assured and klystron tuning error is eliminated.

These improvements in technique allow a more thorough evaluation of cavity performance. Fig. 10 shows the performance of a WX3622 cavity, a 1Q cavity and the performance of a cavity exhibiting pronounced hysteresis, such as might be expected in a diaphragm cavity. The amount of hysteresis in a diaphragm cavity varies and is related to the amount of movement in temperature cycling that occurs. Compensation better than 0.1 mc can be achieved over the temperature range from  $-55^{\circ}\text{C}$  to  $+71^{\circ}\text{C}$ . This includes hysteresis effects. The second curve also represents the performance of a tungsten strut diaphragm cavity. The difference in performance is due to diaphragm setting. A great deal of time was spent in studying and eliminating long term drift in these cavities. Originally, glassed Kovar washers soft soldered to the body were used as windows for the coupling holes. Temperature cycling cavities with these windows produced a negative frequency shift or set each cycle, always occurring after a cold ( $-55^{\circ}\text{C}$ ) cycle. Apparently the soft solder joint was sufficiently hard at the cold temperature to firmly bond the Kovar washer to the copper body and pre-

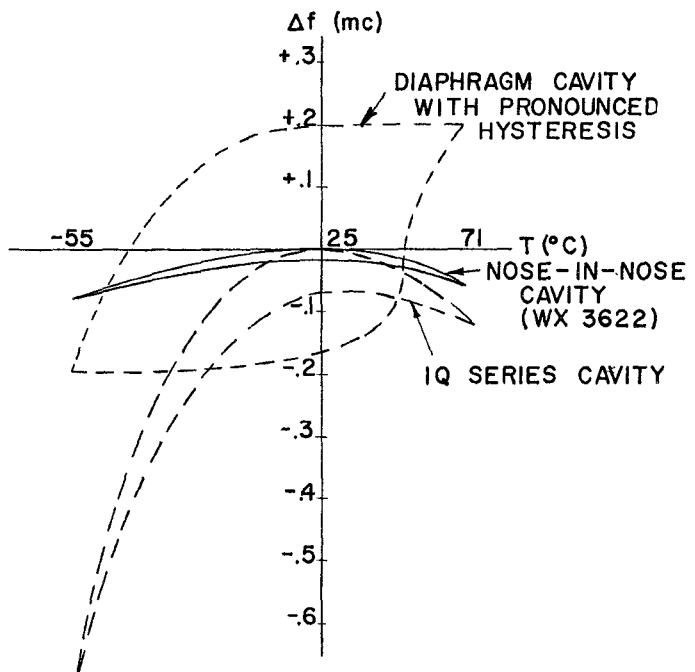


Fig. 10—Cavity compensation.

vent its normal contraction. The result was a net outward distortion of the copper body. At higher temperatures the solder was soft enough to yield and no strain was transmitted to the copper body. This phenomenon was traced up to 25 cycles. By eliminating the Kovar and substituting a copper washer and a resin to glass joint, the soft solder no longer affected the cavity stability. Cavities have been cycled up to 50 cycles from  $100^{\circ}$  to  $-55^{\circ}\text{C}$  with less than 0.1 mc change in room temperature frequency. Most of this occurs in the first few cycles and some sort of aging is required before the cavity is judged to be stable.

#### ACKNOWLEDGMENT

I wish to acknowledge the assistance of R. G. Larson who shared the development. E. C. Okress and W. R. Hayter, Jr., provided help with the theory used to describe the cavity and offered many valuable suggestions. I wish to thank D. E. Marshall for his guidance especially during the uncertain phases of the development.

